

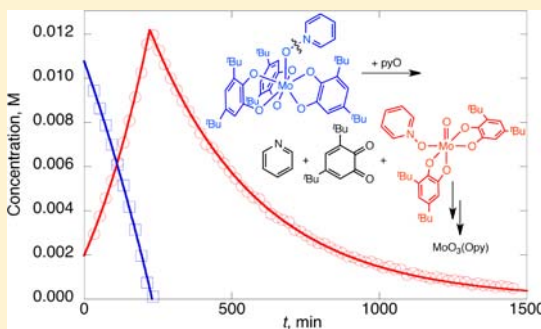
# Tris(3,5-di-*tert*-butylcatecholato)molybdenum(VI): Lewis Acidity and Nonclassical Oxygen Atom Transfer Reactions

Amanda H. Randolph, Nicholas J. Seewald, Karl Rickert, and Seth N. Brown\*

Department of Chemistry and Biochemistry, University of Notre Dame, 251 Nieuwland Science Hall, Notre Dame, Indiana 46556-5670, United States

## Supporting Information

**ABSTRACT:** In the solid state, tris(3,5-di-*tert*-butylcatecholato)-molybdenum(VI) forms a dimer with seven-coordinate molybdenum and bridging catecholates. NMR spectroscopy indicates that the dimeric structure is retained in solution. The molybdenum center has a high affinity for Lewis bases such as pyridine or pyridine-*N*-oxide, forming seven-coordinate monomers with a capped octahedral geometry, as illustrated by the solid-state structure of (3,5-<sup>t</sup>Bu<sub>2</sub>Cat)<sub>3</sub>Mo(py). Structural data indicate that the complexes are best considered as Mo(VI) with substantial  $\pi$  donation from the nonbridging catecholates to molybdenum. Both the dimeric and the monomeric tris(catecholates) react rapidly with water to form free catechol and oxomolybdenum bis(catecholate) complexes. Monooxomolybdenum complexes are also obtained, more slowly, on reaction with dioxygen, with organic products consisting mostly of 3,5-di-*tert*-butyl-1,2-benzoquinone with minor amounts of the extradiol oxidation product 4,6-di-*tert*-butyl-1-oxacyclohepta-4,6-diene-2,3-dione. The pyridine-*N*-oxide complex reacts on heating (with excess pyO) to form initially (3,5-<sup>t</sup>Bu<sub>2</sub>Cat)<sub>2</sub>MoO(Opy) and ultimately MoO<sub>3</sub>(Opy), with quinone and free pyridine as the only organic products. The decay of (3,5-<sup>t</sup>Bu<sub>2</sub>Cat)<sub>3</sub>Mo(Opy) shows an accelerated, autocatalytic profile because the oxidation of its product, (3,5-<sup>t</sup>Bu<sub>2</sub>Cat)<sub>2</sub>Mo(Opy), produces an oxo-rich, catecholate-poor intermediate which rapidly conproportionates with (3,5-<sup>t</sup>Bu<sub>2</sub>Cat)<sub>3</sub>Mo(Opy), providing an additional pathway for its conversion to the mono-oxo product. The tris(catecholate) fragment Mo(3,5-<sup>t</sup>Bu<sub>2</sub>Cat)<sub>3</sub> deoxygenates Opy in this nonclassical oxygen atom transfer reaction slightly less rapidly than does its oxidized product, MoO(3,5-<sup>t</sup>Bu<sub>2</sub>Cat)<sub>2</sub>.



## INTRODUCTION

Catecholates are electron-rich ligands whose redox activity, specifically oxidation to semiquinones and quinones, forms a cornerstone of their chemistry.<sup>1</sup> Further oxidation involving C–C bond cleavage is also possible. For example, catechol-1,2-dioxygenases cleave the bond either between the carbons bonded to oxygen (intradiol oxidation) or adjacent to the catechol moiety (extradiol oxidation).<sup>2</sup> Poly(catecholate) complexes can be efficient catalysts for the aerobic oxidation of catechols, with mixtures of quinones as well as intradiol and extradiol oxidation products being formed.<sup>3,4</sup>

Catecholate ligands can potentially be applied as electron reservoirs to enable redox chemistry at normally redox-inert metal centers.<sup>5</sup> Such inner-sphere redox events, in which the electrons originate in the ligands but the bonding changes take place at the metal center, have been referred to as “non-classical.” We recently elucidated an example of such a nonclassical oxygen atom transfer reaction in the oxidation of oxomolybdenum(VI) bis(3,5-di-*tert*-butylcatecholate) complexes using pyridine-*N*-oxide.<sup>6</sup> Dioxygen is of considerable interest as an oxygen atom transfer reagent in these kinds of reactions, but (3,5-<sup>t</sup>Bu<sub>2</sub>Cat)<sub>2</sub>MoO(L) complexes are inert to O<sub>2</sub>.<sup>6</sup>

In contrast, Cass and Pierpont reported in 1986 that tris(3,5-di-*tert*-butylcatecholato)molybdenum(VI) reacts avidly with dioxygen to give 3,5-di-*tert*-butyl-1,2-benzoquinone and the oxobis(catecholato)molybdenum(VI) dimer Mo<sub>2</sub>O<sub>2</sub>(3,5-<sup>t</sup>Bu<sub>2</sub>Cat)<sub>4</sub>.<sup>7</sup> This represents a formal four-electron nonclassical redox reaction, and we were thus interested in investigating its mechanism. Here we report the results of our study of the chemistry of tris(3,5-di-*tert*-butylcatecholato)-molybdenum(VI). We find that this fragment is quite Lewis acidic, with isolable compounds invariably displaying seven-coordinate at molybdenum. Interaction with a simple oxygen atom transfer agent such as pyridine-*N*-oxide does result in clean oxidation of catecholate to quinone, but reactions with dioxygen are more complex.

## EXPERIMENTAL SECTION

Unless otherwise noted, all procedures were carried out under an inert atmosphere in a nitrogen-filled glovebox or on a vacuum line. When dry solvents were needed, chlorinated solvents and acetonitrile were dried over 4 Å molecular sieves, followed by CaH<sub>2</sub>. Benzene and toluene were dried over sodium. Anhydrous pyridine was purchased from Aldrich and stored in the drybox before use without further

Received: July 5, 2013

Published: October 22, 2013

drying. Deuterated solvents were obtained from Cambridge Isotope Laboratories, dried using the same procedures as their protio analogues, and stored in the drybox prior to use. Pyridine-*N*-oxide (Acros) was sublimed under reduced pressure and stored in the drybox. All other reagents were commercially available and used without further purification. NMR spectra were measured on Varian VXR-300, Varian VXR-500, or Bruker DPX-400 spectrometers. Chemical shifts for  $^1\text{H}$  and  $^{13}\text{C}\{^1\text{H}\}$  spectra are reported in ppm downfield of TMS, with spectra referenced using the known chemical shifts of the solvent residuals. Infrared spectra ( $4000\text{--}600\text{ cm}^{-1}$ ) were recorded as Nujol mulls on a JASCO FT/IR-6300 spectrometer. Elemental analyses were performed by Midwest Microlab, LLC (Indianapolis, IN).

**Hexakis(3,5-di-*tert*-butylcatecholato)dimolybdenum(VI),  $\text{Mo}_2(3,5\text{-}^t\text{Bu}_2\text{Cat})_6$ .** *Method A. From Tricarbonyl(cycloheptatriene)molybdenum(0).* In the drybox, (cycloheptatriene)molybdenum tricarbonyl (0.325 g, 1.19 mmol, Aldrich) was dissolved in 18 mL of benzene. In a separate vial, 3,5-di-*tert*-butyl-1,2-benzoquinone (0.821 g, 3.73 mmol, Aldrich) was dissolved in 4 mL of benzene. The solutions were added to a 50 mL Erlenmeyer flask, and the solution was stirred for 1 h. On mixing, the solution frothed vigorously for 5 min and turned dark blue, depositing a fine blue precipitate. The solid was filtered on a glass frit and washed with hexanes to give 0.734 g of  $\text{Mo}_2(3,5\text{-}^t\text{Bu}_2\text{Cat})_6$  (81%) as fine blue microcrystals.  $^1\text{H}$  NMR (300 MHz,  $\text{CDCl}_3$ ,  $20\text{ }^\circ\text{C}$ ):  $\delta$  1.29 (s, 54H,  $^t\text{Bu}$ ), 1.38 (s, 54H,  $^t\text{Bu}$ ), 6.77 (br s, 6H, ArH), 7.38 (br s, 6H, ArH). IR ( $\text{cm}^{-1}$ ): 1584 (s), 1549 (m), 1409 (w), 1395 (w), 1385 (m), 1362 (s), 1298 (m), 1254 (m), 1226 (s), 1201 (s), 1187 (m), 1175 (w), 1100 (m), 1029 (m), 993 (s), 978 (s), 915 (m), 875 (w), 856 (s), 837 (s), 813 (w), 774 (w), 767 (w), 754 (m), 745 (w), 692 (s), 655 (m), 631 (s). The analytical sample retained two moles of benzene per dimer. Anal. Calcd for  $\text{C}_{96}\text{H}_{132}\text{Mo}_2\text{O}_{12}$ : C, 69.04; H, 7.97. Found: C, 68.53; H, 7.50.

*Method B. From Molybdenum Hexacarbonyl.* In the drybox,  $\text{Mo}(\text{CO})_6$  (0.598 g, 2.27 mmol, Aldrich) and 3,5-di-*tert*-butyl-1,2-benzoquinone (1.506 g, 6.84 mmol, Aldrich) were added to a glass bomb with a Teflon valve. The valve was sealed and the bomb removed from the drybox. Dry benzene (20 mL) was added to the bomb with vacuum transfer. The solution was heated in an  $85\text{ }^\circ\text{C}$  oil bath, with stirring, for 24 h. The glass bomb was allowed to cool to room temperature and brought back into the drybox. The solution was filtered through a glass frit, and the solid was washed with hexanes and dried under vacuum 45 min to furnish large dark blue crystals of  $\text{Mo}_2(3,5\text{-}^t\text{Bu}_2\text{Cat})_6$  (0.613 g, 36%).

**Tris(3,5-di-*tert*-butylcatecholato)(pyridine)molybdenum(VI),  $(3,5\text{-}^t\text{Bu}_2\text{Cat})_3\text{Mo}(\text{py})$ .** In the drybox,  $\text{Mo}_2(3,5\text{-}^t\text{Bu}_2\text{Cat})_6$  (98.5 mg, 0.130 mmol Mo) was dissolved in dry acetonitrile (2.0 mL) containing excess pyridine (32.3  $\mu\text{L}$ ). After one week, large bronze crystals of  $(3,5\text{-}^t\text{Bu}_2\text{Cat})_3\text{Mo}(\text{py})$  were isolated by filtration through a glass frit. After washing with acetonitrile, the yield of the pyridine adduct was 42.0 mg (39%).  $^1\text{H}$  NMR ( $\text{C}_6\text{D}_6$ ):  $\delta$  1.26 (s, 27H,  $^t\text{Bu}$ ), 1.38 (s, 27H,  $^t\text{Bu}$ ), 6.53 (t, 7 Hz, 2H, py 3,5-H), 6.80 (t, 7 Hz, 1H, py 4-H), 7.09 (s, 3H, ArH), 7.16 (s, 3H, ArH), 9.15 (d, 5 Hz, 2H, py 2,6-H).  $^{13}\text{C}\{^1\text{H}\}$  NMR ( $\text{C}_6\text{D}_6$ ):  $\delta$  30.40, 32.26 ( $\text{C}(\text{CH}_3)_3$ ), 35.12, 35.39 ( $\text{C}(\text{CH}_3)_3$ ), 111.35, 118.87, 124.53, 137.07, 139.21, 147.82, 151.08, 160.89, 163.43. IR ( $\text{cm}^{-1}$ ): 1587 (s), 1552 (w), 1362 (s), 1298 (s), 1252 (w), 1232 (s), 1209 (s), 1100 (w), 1069 (m), 1022 (m), 983 (s), 938 (w), 913 (w), 850 (w), 835 (w), 761 (m), 722 (w). Anal. Calcd for  $\text{C}_{47}\text{H}_{65}\text{MoNO}_6$ : C, 67.53; H, 7.84; N, 1.68. Found: C, 67.37; H, 7.64; N, 1.90.

**Tris(3,5-di-*tert*-butylcatecholato)(pyridine-*N*-oxide)molybdenum(VI),  $(3,5\text{-}^t\text{Bu}_2\text{Cat})_3\text{Mo}(\text{Opy})$ .** This compound was generated in situ by addition of pyridine-*N*-oxide (3.4 mg) to  $\text{Mo}_2(3,5\text{-}^t\text{Bu}_2\text{Cat})_6$  (20.8 mg) in 0.7 mL of deuterated solvent.  $^1\text{H}$  NMR ( $\text{C}_6\text{D}_6$ ):  $\delta$  1.29 (s, 27H,  $^t\text{Bu}$ ), 1.43 (s, 27H,  $^t\text{Bu}$ ), 6.21 (t, 7 Hz, 2H, Opy 3,5-H), 6.41 (t, 8 Hz, 1H, Opy 4-H), 6.93 (d, 2 Hz, 3H, ArH), 7.12 (d, 2 Hz, 3H, ArH), 8.27 (d, 6 Hz, 2H, Opy 2,6-H).  $^{13}\text{C}\{^1\text{H}\}$  NMR ( $\text{C}_6\text{D}_6$ ):  $\delta$  30.52, 32.40 ( $\text{C}(\text{CH}_3)_3$ ), 35.05, 35.43 ( $\text{C}(\text{CH}_3)_3$ ), 110.45, 117.93, 125.38 (Opy 3,5-C), 128.68 (Opy 4-C), 136.65, 142.88 (Opy 2,6-C), 146.93, 161.02, 162.73.

**Generation of Alternative Isomer of  $\text{Mo}_2\text{O}_2(3,5\text{-}^t\text{Bu}_2\text{Cat})_4$  (1b) by Reaction of  $3,5\text{-}^t\text{Bu}_2\text{CatH}_2$  with  $\text{MoO}_2(\text{acac})_2$ .** In a screw-cap NMR tube in the drybox, 19.0 mg of  $\text{MoO}_2(\text{acac})_2$  (Strem, 58.3  $\mu\text{mol}$ ) and 26.3 mg of 3,5-di-*tert*-butylcatechol (Aldrich, 118  $\mu\text{mol}$ , 2.03 equiv) were dissolved in 0.6 mL of  $\text{CDCl}_3$ . The dark purple solution contained roughly equal quantities of the Buchanan–Pierpont isomer of  $\text{Mo}_2\text{O}_2(3,5\text{-}^t\text{Bu}_2\text{Cat})_4$  (1a)<sup>8</sup> ( $^1\text{H}$  NMR of 1a:  $\delta$  0.90, 1.26, 1.29, 1.53 [s, 18H ea.,  $^t\text{Bu}$ ], 6.39, 6.77, 7.03, 7.19 [d, 2 Hz, 2H ea., ArH])<sup>4</sup> and a previously unobserved isomer of the dimer (1b).  $^1\text{H}$  NMR of 1b ( $\text{CDCl}_3$ ):  $\delta$  0.98, 1.28, 1.31, 1.54 (s, 18H ea.,  $^t\text{Bu}$ ), 6.67, 6.80, 7.11, 7.20 (d, 2 Hz, 2H ea., ArH).

**Variable-Temperature NMR Spectroscopy of  $(3,5\text{-}^t\text{Bu}_2\text{Cat})_3\text{Mo}(\text{py})$ .** NMR spectra were recorded between  $-70\text{ }^\circ\text{C}$  and  $+50\text{ }^\circ\text{C}$  in toluene- $d_8$  on a Varian VXR-500 NMR spectrometer. To calculate exchange rates, the pyridine resonances were simulated using the program gNMR,<sup>9</sup> and the calculated lineshapes were superimposed on the observed spectra. Activation parameters for the exchange reaction were calculated by plotting  $\ln(k_{\text{diss}}/T)$  vs  $1/T$ .

**Kinetics of Reactions of  $(3,5\text{-}^t\text{Bu}_2\text{Cat})_3\text{Mo}(\text{Opy})$  in Toluene- $d_8$ .** In a typical reaction, 6.4 mg of  $\text{Mo}_2(3,5\text{-}^t\text{Bu}_2\text{Cat})_6$  and 3.6 mg of 1,4-bis(trimethylsilyl)benzene (used as an internal standard) were dissolved in 0.70 mL of a stock 0.102 M solution of pyridine-*N*-oxide in  $\text{C}_6\text{D}_5\text{CD}_3$  in a screw-cap NMR tube in the drybox. (Use of a greater excess of pyridine-*N*-oxide is precluded by its limited solubility in toluene.) The tube was sealed with a Teflon-lined cap and stored in a  $-20\text{ }^\circ\text{C}$  freezer until ready for use. The Varian VXR-500 probe was preheated to  $70\text{ }^\circ\text{C}$  with a dummy sample, then the actual sample tube was inserted into the preheated probe. After locking and shimming, spectra were acquired every 20 min for 24 h, and concentrations of the various species were determined by integration of the *tert*-butyl resonances against the trimethylsilyl peak of the internal standard. Concentration vs time profiles were fit to the Supporting Information, eq S5 (for  $[(3,5\text{-}^t\text{Bu}_2\text{Cat})_3\text{Mo}(\text{Opy})]$ ) and Supporting Information, eqs S6–S7 (for  $[(3,5\text{-}^t\text{Bu}_2\text{Cat})_2\text{Mo}(\text{Opy})]$ ) using the program Kaleidagraph (Synergy Software, v. 4.1). In the data fitting, the total Mo concentration ( $[(3,5\text{-}^t\text{Bu}_2\text{Cat})_3\text{Mo}(\text{Opy})] + [(3,5\text{-}^t\text{Bu}_2\text{Cat})_2\text{Mo}(\text{Opy})]$  before the disappearance of  $(3,5\text{-}^t\text{Bu}_2\text{Cat})_3\text{Mo}(\text{Opy})$ ) was fixed at its average value over this time period, with the initial concentration of  $(3,5\text{-}^t\text{Bu}_2\text{Cat})_3\text{Mo}(\text{Opy})$  ( $\text{Mo}_0$ ) and the rate constants  $k_1$  and  $k_2$  the only adjustable parameters in the fits.

**X-ray Crystallography.** Crystals of  $\text{Mo}_2(3,5\text{-}^t\text{Bu}_2\text{Cat})_6 \cdot 4\text{ C}_6\text{D}_6$  were grown by slowly cooling the reaction mixture of 3,5-di-*tert*-butyl-1,2-benzoquinone with  $\text{Mo}(\text{CO})_6$  in  $\text{C}_6\text{D}_6$  in a sealed NMR tube. Crystals of  $(3,5\text{-}^t\text{Bu}_2\text{Cat})_3\text{Mo}(\text{py}) \cdot \text{CH}_3\text{CN}$  were grown by diffusion of acetonitrile into a benzene solution of the complex. Crystals were placed in Paratone oil before being transferred to the cold  $\text{N}_2$  stream of a Bruker Apex II CCD diffractometer in a nylon loop. Data were reduced, correcting for absorption, using the program SADABS. The structures were solved using a Patterson map to find the molybdenum atoms and the atoms in the first coordination sphere, with other heavy atoms found on subsequent difference Fourier maps. All nonhydrogen atoms were refined anisotropically.

The *tert*-butyl group in  $(3,5\text{-}^t\text{Bu}_2\text{Cat})_3\text{Mo}(\text{py}) \cdot \text{CH}_3\text{CN}$  centered on C18 was disordered in two different orientations. The disorder was modeled by constraining the thermal parameters of opposite carbons to be equal and allowing the two orientations' occupancies to refine (the major component of the disorder was found to have an occupancy of 80.0(6)%). Hydrogen atoms in the disordered *tert*-butyl group of  $(3,5\text{-}^t\text{Bu}_2\text{Cat})_3\text{Mo}(\text{py}) \cdot \text{CH}_3\text{CN}$  were placed in calculated positions. All other hydrogen (and deuterium) atoms were found on difference Fourier maps and refined isotropically. Calculations used SHELXTL (Bruker AXS),<sup>10</sup> with scattering factors and anomalous dispersion terms taken from the literature.<sup>11</sup> Further details about the structures are given in Table 1.

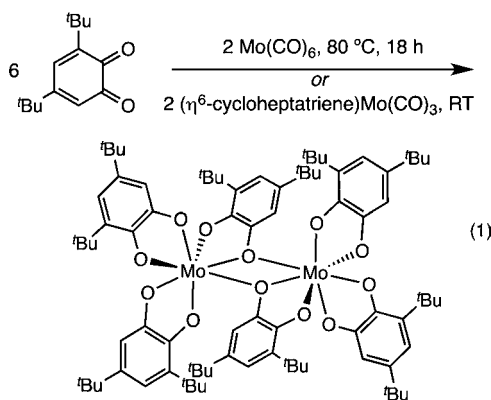
## RESULTS

**Preparation and Structure of Homoleptic Molybdenum(VI) Tris(3,5-di-*tert*-butylcatecholate).** Cass and Pierpont reported in 1986 that  $\text{Mo}(3,5\text{-}^t\text{Bu}_2\text{Cat})_3$  is formed

**Table 1.** Crystal data for  $\text{Mo}_2(3,5\text{-}^t\text{Bu}_2\text{Cat})_6\cdot 4\text{C}_6\text{D}_6$  and  $(3,5\text{-}^t\text{Bu}_2\text{Cat})_3\text{Mo}(\text{py})\cdot \text{CH}_3\text{CN}$ 

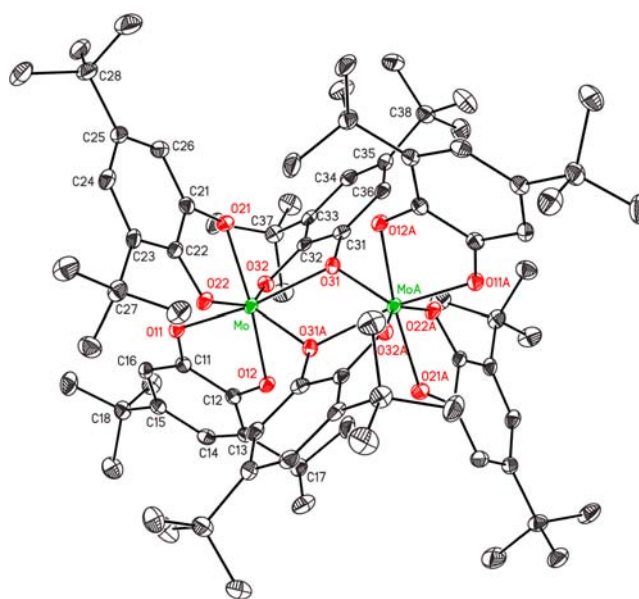
	$\text{Mo}_2(3,5\text{-}^t\text{Bu}_2\text{Cat})_6\cdot 4\text{C}_6\text{D}_6$	$(3,5\text{-}^t\text{Bu}_2\text{Cat})_3\text{Mo}(\text{py})\cdot \text{CH}_3\text{CN}$
empirical formula	$\text{C}_{108}\text{H}_{120}\text{D}_{24}\text{Mo}_2\text{O}_{12}$	$\text{C}_{49}\text{H}_{68}\text{MoN}_2\text{O}_6$
temperature (K)	100(2)	120(2)
$\lambda$ (Å)	0.71073 (Mo $K\alpha$ )	0.71073 (Mo $K\alpha$ )
space group	$P\bar{1}$	$P\bar{1}$
total data collected	28023	27516
no. of indep reflns.	9860	9535
$R_{\text{int}}$	0.0546	0.0556
obsd. refls. [ $I > 2\sigma(I)$ ]	7680	7159
$a$ (Å)	13.9365(12)	10.5873(17)
$b$ (Å)	14.7478(13)	12.436(2)
$c$ (Å)	15.1427(14)	18.282(3)
$\alpha$ (deg)	116.0609(17)	91.913(4)
$\beta$ (deg)	91.5854(16)	95.778(4)
$\gamma$ (deg)	114.6777(15)	101.514(4)
$V$ (Å <sup>3</sup> )	2454.1(4)	2343.1(7)
$Z$	1	2
cryst size (mm)	$0.13 \times 0.10 \times 0.03$	$0.41 \times 0.12 \times 0.10$
no. refined params.	838	805
R indices [ $I > 2\sigma(I)$ ]	$R1 = 0.0417,$ $wR2 = 0.0784$	$R1 = 0.0419,$ $wR2 = 0.0834$
R indices (all data)	$R1 = 0.0634,$ $wR2 = 0.0864$	$R1 = 0.0701,$ $wR2 = 0.0929$
goodness of fit	1.017	1.012

on heating  $\text{Mo}(\text{CO})_6$  with 3,5-di-*tert*-butyl-1,2-benzoquinone in toluene under anaerobic conditions.<sup>7</sup> We find that this reaction is conveniently carried out in benzene, from which dark blue crystals of a benzene solvate of the compound deposit on cooling (eq 1). The same compound forms immediately at



room temperature if the quinone is allowed to react with  $(\eta^6\text{-cycloheptatriene})\text{molybdenum}$  tricarbonyl, and precipitates from benzene as a fine powder. The low reactivity of  $\text{Mo}(\text{CO})_6$  as a  $\text{Mo}(0)$  source has been documented previously in the formation of a molybdenum tris(catecholate) complex from 1,10-phenanthroline-5,6-dione, where  $\text{Mo}(\eta^6\text{-C}_6\text{H}_5\text{CH}_3)_2$  was found to be more reactive than  $\text{Mo}(\text{CO})_6$ .<sup>12</sup>

While it was originally formulated as a six-coordinate monomer,<sup>7</sup> the tris(catecholate) complex in fact exists in the solid state as a seven-coordinate dimer with a pair of bridging catecholates (Figure 1). Each bridging catecholate has the oxygen *ortho* to the *tert*-butyl group (O32) bonded solely to one molybdenum, with the less hindered oxygen bridging the molybdenum atoms in a relatively symmetric fashion ( $\text{Mo}-$

**Figure 1.** Thermal ellipsoid plot (50% ellipsoids) of the metal complex in  $\text{Mo}_2(3,5\text{-}^t\text{Bu}_2\text{Cat})_6\cdot 4\text{C}_6\text{D}_6$ . Hydrogen atoms are omitted for clarity.

$\text{O31} = 2.0932(17)$  Å,  $\text{Mo}-\text{O31A} = 2.1108(17)$  Å, Table 2). The same connectivity is observed in the bridging catecholates of the oxomolybdenum dimer  $\text{Mo}_2\text{O}_2(3,5\text{-}^t\text{Bu}_2\text{Cat})_4$ , but in the oxomolybdenum complex the bridging catecholates are steeply inclined with respect to the  $\text{Mo}_2\text{O}_2$  plane ( $124.2^\circ$  angle between planes).<sup>8</sup> In contrast, the bridging catecholates of the homoleptic dimer are roughly in the  $\text{Mo}_2\text{O}_2$  plane ( $29.5^\circ$  angle between planes), a much more typical arrangement for metal complexes containing a bis( $\mu$ -3,5-di-*tert*-butylcatecholate) motif.<sup>13</sup>

Seven-coordinate tris(chelate) complexes of molybdenum or tungsten with small bite-angle chelates such as 2-mercaptopyridine<sup>14</sup> or dithiocarbamate<sup>15</sup> adopt structures that are well described as pentagonal bipyramids with two equatorial chelates and one chelate that spans the equatorial and axial positions. An oxomolybdenum catecholate complex  $\text{MoO}(\text{C}_5\text{H}_{10}\text{NO})_2(\text{cat})$  with a nominally pentagonal bipyramidal geometry, if the  $\eta^2$ -piperidinolato ligands are counted as occupying two coordination sites, has also been reported.<sup>16</sup> The molybdenum in  $\text{Mo}_2(3,5\text{-}^t\text{Bu}_2\text{Cat})_6$  does not adopt a pentagonal bipyramidal geometry, possibly because of the somewhat larger bite angle of catecholate ( $\sim 76^\circ$ ) compared with that of dithiocarbamate ( $\sim 70^\circ$ ) or 2-mercaptopyridine ( $\sim 65^\circ$ ), or piperidinolate ( $\sim 35^\circ$ ). The geometry of the Mo center in the dimer is rather irregular and is not well described by any of the usual idealized seven-coordinate geometries (capped octahedron, capped trigonal prism, 4:3 piano stool).<sup>17</sup>

High-valent molybdenum complexes usually have oxo or other strong  $\pi$ -donor ligands, a class to which catecholates potentially belong.<sup>18</sup> Since  $\pi$  donation depletes electron density in the catecholate highest occupied molecular orbital (HOMO), just as ligand oxidation to the semiquinone does, the extent of  $\pi$  donation in catecholates can be assessed by calculating an apparent "metrical" oxidation state (MOS) of the ligand based on the carbon-carbon and carbon-oxygen distances.<sup>19</sup> A noninteger MOS is particularly indicative of partial transfer of electron density via  $\pi$  donation, rather than outright electron transfer. Noninteger MOS values are observed in the chelating ligands in  $\text{Mo}_2(3,5\text{-}^t\text{Bu}_2\text{Cat})_6$ , which have MOS

**Table 2. Selected Bond Distances (Å) and Angles (deg) for the First Coordination Spheres in  $\text{Mo}_2(3,5\text{-}^t\text{Bu}_2\text{Cat})_6\cdot 4\text{C}_6\text{D}_6$  and  $(3,5\text{-}^t\text{Bu}_2\text{Cat})_3\text{Mo}(\text{py})\cdot\text{CH}_3\text{CN}$**

	$\text{Mo}_2(3,5\text{-}^t\text{Bu}_2\text{Cat})_6\cdot 4\text{C}_6\text{D}_6$	$(3,5\text{-}^t\text{Bu}_2\text{Cat})_3\text{Mo}(\text{py})\cdot\text{CH}_3\text{CN}$
Mo–O11	1.9729(17)	1.9767(19)
Mo–O12	2.0017(16)	1.9792(18)
Mo–O21	1.9876(17)	2.0030(18)
Mo–O22	1.9827(16)	1.9731(18)
Mo–O31	2.0932(17)	1.9893(18)
Mo–O32	1.9617(17)	1.9987(18)
Mo–O31A	2.1113(17)	
Mo–N		2.274(2)
O11–Mo–O12	76.76(7)	77.06(7)
O21–Mo–O22	75.67(7)	76.07(7)
O31–Mo–O32	75.53(7)	75.98(7)
O11–Mo–O21	90.98(7)	84.11(7)
O11–Mo–O22	84.19(7)	110.86(8)
O11–Mo–O31	156.80(7)	157.91(7)
O11–Mo–O32	81.75(7)	109.32(7)
O11–Mo–O31A	133.23(7)	
O11–Mo–N		76.86(8)
O12–Mo–O21	160.41(7)	81.28(7)
O12–Mo–O22	117.39(7)	154.86(7)
O12–Mo–O31	104.23(7)	82.98(7)
O12–Mo–O32	81.90(7)	80.15(7)
O12–Mo–O31A	73.99(6)	
O12–Mo–N		131.08(8)
O21–Mo–O31	81.09(7)	83.59(7)
O21–Mo–O32	81.25(7)	153.82(7)
O21–Mo–O31A	124.77(7)	
O21–Mo–N		135.39(8)
O22–Mo–O31	114.42(7)	83.78(7)
O22–Mo–O32	152.67(7)	117.01(7)
O22–Mo–O31A	78.01(7)	
O22–Mo–N		73.83(8)
O31–Mo–O31A	67.24(7)	
O31–Mo–N		124.26(8)
O32–Mo–O31A	128.08(7)	
O32–Mo–N		70.62(7)
Mo–O31–Mo0A	112.76(7)	

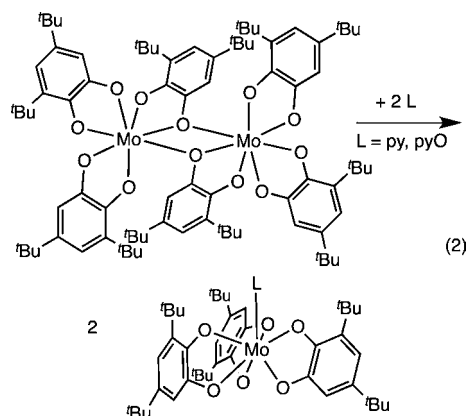
values of  $-1.66(12)$  and  $-1.67(14)$  for rings 1 and 2, respectively. The bridging catecholate shows bond distances typical of fully reduced catecholates with little  $\pi$  bonding,  $\text{MOS} = -2.00(16)$ . The nonbridging catecholates are similar to those *trans* to oxo in  $\text{MoO}(\text{cat})_2(\text{L})$  ( $\text{cat} = 3,6\text{-}^t\text{Bu}_2\text{Cat}$ ,  $\text{L} = \text{ONC}_5\text{H}_5$ ,  $\text{OSMe}_2$ ,  $\text{OAsPh}_3$ ,  $\text{MOS} = -1.63(7)$ ;<sup>20</sup>  $\text{cat} = 3,5\text{-}^t\text{Bu}_2\text{Cat}$ ,  $\text{L} = \text{ONC}_5\text{H}_4\text{-4-CH}_3$ ,  $\text{MOS} = -1.56(9)$ <sup>6</sup>), which are able to donate into a single  $d\pi$  orbital that is not engaged in  $\pi$  bonding with the oxo group. Likewise, the seven-coordinate molybdenum in  $\text{Mo}_2(3,5\text{-}^t\text{Bu}_2\text{Cat})_6$  is expected to have two  $d$  orbitals available for  $\pi$  bonding, allowing each of the nonbridging catecholates to donate into one  $d\pi$  orbital.

At room temperature in noncoordinating solvents such as  $\text{C}_6\text{D}_5\text{CD}_3$  or  $\text{CD}_2\text{Cl}_2$ , the  $^1\text{H}$  NMR spectrum of  $\text{Mo}_2(3,5\text{-}^t\text{Bu}_2\text{Cat})_6$  shows broad resonances in both the *tert*-butyl and the aromatic regions. Cooling solutions in  $\text{CD}_2\text{Cl}_2$  causes the resonances to decoalesce into a very complex spectrum with no fewer than nine distinct environments for the catecholate ligands. Since monomeric  $\text{Mo}(3,5\text{-}^t\text{Bu}_2\text{Cat})_3$  would exhibit no more than four distinct environments (one for the

$\text{C}_3$ -symmetric octahedral isomer and three for the  $\text{C}_1$ -symmetric isomer), the large number of distinct environments observed strongly suggests that a dimeric structure is largely retained in solution. (While the solid-state structure would give only three catecholate environments, isomerism involving different orientations of the nonbridging catecholates is likely and could give rise to up to 16 stereoisomers.) The spectrum in  $\text{CD}_2\text{Cl}_2$  is sharp at  $-30^\circ\text{C}$  and essentially unchanged upon further cooling, which makes the presence of significant amounts of monomer unlikely at these temperatures, since the monomer–dimer equilibrium would be expected to be highly temperature-dependent. The observed coalescence of resonances into a single catecholate environment at temperatures above  $30^\circ\text{C}$  (at 500 MHz) indicates that dissociation to monomers is likely thermally accessible.

#### Reactions of $\text{Mo}_2(3,5\text{-}^t\text{Bu}_2\text{Cat})_6$ with Lewis Bases.

Addition of pyridine or pyridine-*N*-oxide to solutions of  $\text{Mo}_2(3,5\text{-}^t\text{Bu}_2\text{Cat})_6$  results in an immediate color change from dark blue-violet to dark royal blue (pyridine) or electric blue (pyridine-*N*-oxide).  $^1\text{H}$  NMR spectra reveal new signals due to bound pyridine or pyridine-*N*-oxide (in a mole ratio of 1:3 relative to the catecholates), and aromatic doublets and *tert*-butyl singlets due to a single type of 3,5-di-*tert*-butylcatecholate, suggesting the formation of monomeric adducts  $(3,5\text{-}^t\text{Bu}_2\text{Cat})_3\text{Mo}(\text{L})$  (eq 2). NMR spectra at low temperature ( $-70^\circ\text{C}$ ) show little broadening of the catecholate signals, indicating that the adducts formed are either symmetrical or highly fluxional.



Further insight into the nature of these adducts is provided by the solid-state structure of  $(3,5\text{-}^t\text{Bu}_2\text{Cat})_3\text{Mo}(\text{py})$ , which shows a seven-coordinate monomer (Figure 2). Its geometry is a nearly ideal capped octahedron, with the catecholates spanning the vertices of the octahedron and the pyridine binding along the pseudo- $\text{C}_3$  axis. The capped face is significantly expanded ( $\text{O–Mo–O}$  angles  $112(4)^\circ$  avg), resembling tetrahedral geometry, while the opposite face is slightly compressed compared to an ideal octahedral geometry ( $\text{O–Mo–O}$   $82.6(12)^\circ$ ). The  $\text{Mo–N}$  distance ( $2.274(2)$  Å) is typical of pyridines bonded to  $\text{Mo}(\text{VI})$  that are not *trans* to an oxo or imido group ( $2.27(4)$  Å avg, 15 examples).<sup>18,21</sup>

The three catecholates in  $(3,5\text{-}^t\text{Bu}_2\text{Cat})_3\text{Mo}(\text{py})$  also show structural signs of noticeable  $\pi$ -donation ( $\text{MOS} = -1.87(11)$ ,  $-1.73(11)$ , and  $-1.72(14)$  for rings 1–3, respectively). These values are indicative of somewhat less donation than observed for the nonbridging catecholates in  $\text{Mo}_2(3,5\text{-}^t\text{Bu}_2\text{Cat})_6$ . This is reasonable since the  $\pi$  donation in both seven-coordinate complexes is into two  $d\pi$  orbitals, but is shared among three

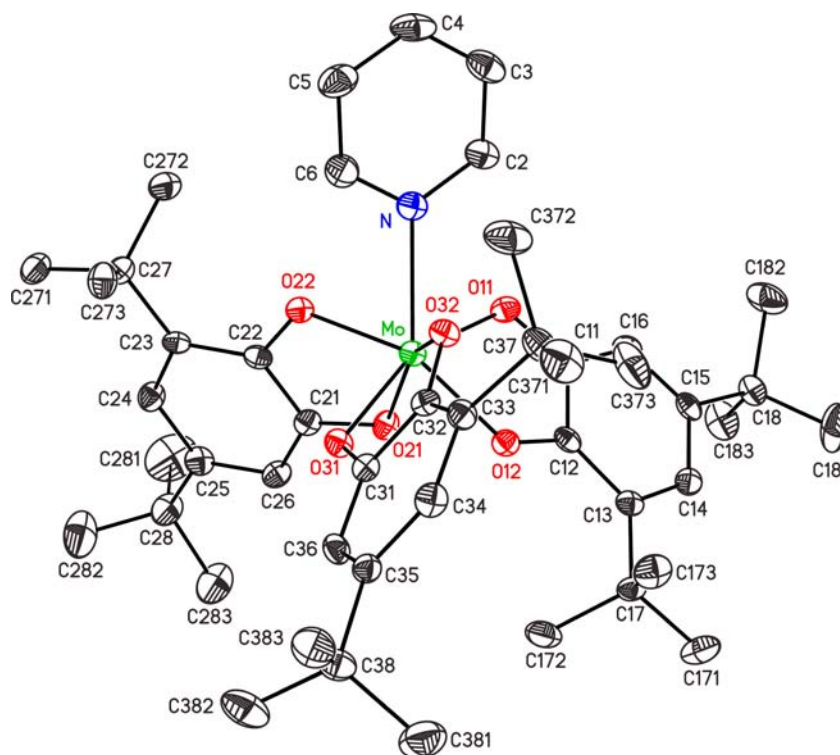
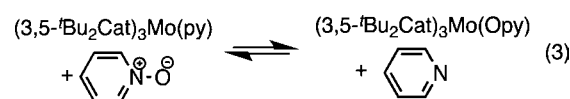


**Figure 2.** Thermal ellipsoid plot (50% ellipsoids) of the metal complex in  $(3,5\text{-}t\text{Bu}_2\text{Cat})_3\text{Mo}(\text{py})\cdot\text{CH}_3\text{CN}$ , with hydrogen atoms omitted for clarity.

catecholates in  $(3,5\text{-}t\text{Bu}_2\text{Cat})_3\text{Mo}(\text{py})$  as opposed to only two in  $\text{Mo}_2(3,5\text{-}t\text{Bu}_2\text{Cat})_6$ . The overall  $\pi$  donation, as judged from the sum of the MOS values of the three catecholates, is very similar in the two complexes ( $\Sigma\text{MOS} = -5.33$  for  $\text{Mo}_2(3,5\text{-}t\text{Bu}_2\text{Cat})_6$  and  $-5.32$  for  $(3,5\text{-}t\text{Bu}_2\text{Cat})_3\text{Mo}(\text{py})$ ). The  $d\pi$  orbitals in the capped octahedral geometry, essentially  $d_{xy}$  and  $d_{x^2-y^2}$  with the Mo–N vector taken as the  $z$  axis, overlap more strongly with the oxygen atoms on the capped face. This may explain why the  $\pi$  interaction appears slightly weaker in catecholate 1 which, uniquely, has its less electron-rich oxygen (O11, *meta* to  $t\text{Bu}$ ) on the capped face. The observation of an unsymmetrical arrangement of *tert*-butyl groups in the solid state suggests that the compound must be fluxional in solution to explain the high symmetry of its NMR spectra.

While the catecholate resonances remain sharp and symmetrical in the NMR at all temperatures observed, resonances due to bound pyridine in  $(3,5\text{-}t\text{Bu}_2\text{Cat})_3\text{Mo}(\text{py})$  do show broadening and coalescence with those of free pyridine (Figure 3). The linewidths of the bound pyridine peaks in the slow-exchange regime are independent of the concentration of free pyridine, indicating the mechanism of exchange involves dissociation of pyridine from molybdenum. This is consistent with the activation parameters obtained by Eyring analysis of the exchange rate constants ( $0\text{--}50\text{ }^\circ\text{C}$ ,  $\Delta H^\ddagger = 15.4 \pm 0.6$  kcal/mol,  $\Delta S^\ddagger = +6.6 \pm 2.0$  cal/mol·K, Supporting Information, Figure S1). Judging from dissociation rates, the Mo- $(3,5\text{-}t\text{Bu}_2\text{Cat})_3$  fragment appears to be less Lewis acidic than the five-coordinate oxomolybdenum(VI) bis(amidophenoxide) fragment  $(t\text{BuClip})\text{MoO}$ , since  $(t\text{BuClip})\text{MoO}(\text{py})$  dissociates pyridine about 10 times more slowly than does  $(3,5\text{-}t\text{Bu}_2\text{Cat})_3\text{Mo}(\text{py})$  at  $22\text{ }^\circ\text{C}$ .<sup>18</sup> The oxobis(catecholate) fragment  $(3,5\text{-}t\text{Bu}_2\text{Cat})_2\text{MoO}$  is qualitatively much more Lewis acidic, since ligand exchange in  $(\text{Cat})_2\text{MoO}(\text{L})$  is relatively slow<sup>20</sup> and does not involve ligand dissociation.<sup>6</sup>

Pyridine-*N*-oxide binds to  $(3,5\text{-}t\text{Bu}_2\text{Cat})_3\text{Mo}$  somewhat more tightly than does pyridine, with  $K_{\text{eq}} = 2.5$  for eq 3 in toluene- $d_6$



at  $0\text{ }^\circ\text{C}$ . Analysis of the temperature-dependence of the equilibrium constant  $K_3$  ( $-70\text{--}0\text{ }^\circ\text{C}$ , Supporting Information, Figure S2) gives  $\Delta H^\circ_3 = -0.69 \pm 0.07$  kcal/mol,  $\Delta S^\circ_3 = -0.8 \pm 0.3$  cal/mol·K.

**Hydrolysis of Tris(catecholate)molybdenum(VI) Complex.** Contrary to preliminary reports,<sup>7</sup> we find all of the tris(catecholato)molybdenum(VI) complexes to be exceptionally moisture-sensitive. In situ monitoring of reactions of  $\text{Mo}_2(3,5\text{-}t\text{Bu}_2\text{Cat})_6$  with excess water by NMR spectroscopy reveals that the complex reacts immediately to form free 3,5-di-*tert*-butylcatechol. The two sets of catecholate resonances characteristic of the oxomolybdenum dimer  $\text{Mo}_2\text{O}_2(3,5\text{-}t\text{Bu}_2\text{Cat})_4$  **1a**, originally reported by Buchanan and Pierpont,<sup>8</sup> and two other sets of catecholate resonances assigned to a hitherto unreported isomer of it, **1b**, are observed (eq 4). Both **1a** and **1b** also form, in similar quantities, on reaction of 3,5-di-*tert*-butylcatechol with  $\text{MoO}_2(\text{acac})_2$  in  $\text{CDCl}_3$ .<sup>22</sup> We have been unable to find conditions to produce **1b** in pure form or to separate it from **1a**. The structure is tentatively assigned to have bridging catecholates *cis* to the oxo group by analogy to the quasi-isostructural  $\text{V}_2\text{O}_2(3,5\text{-}t\text{Bu}_2\text{Cat})_2(3,5\text{-}t\text{Bu}_2\text{SQ})_2$ , where such a structure has recently been observed<sup>13m</sup> in addition to the known isomer analogous to **1a**.<sup>23</sup> If substoichiometric quantities of water are used, a species that displays NMR signals for catecholate ligands in five distinct environments can be observed, which is tentatively assigned as a partially hydrolyzed monooxidimo-

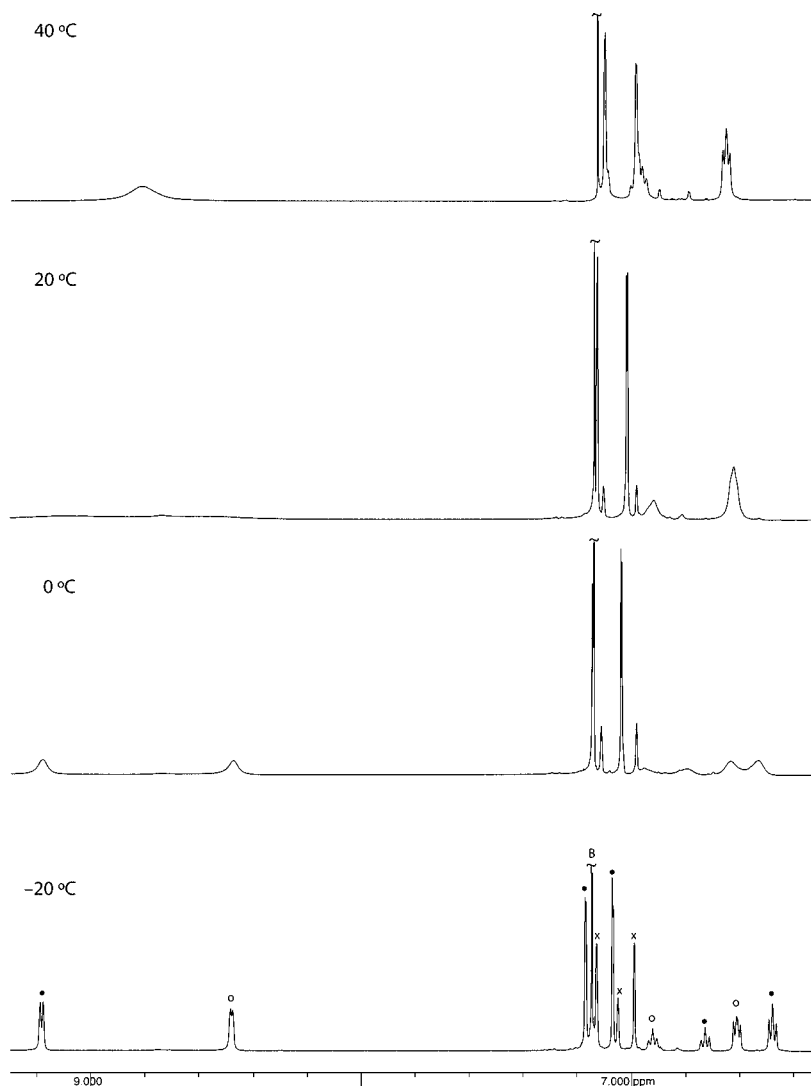
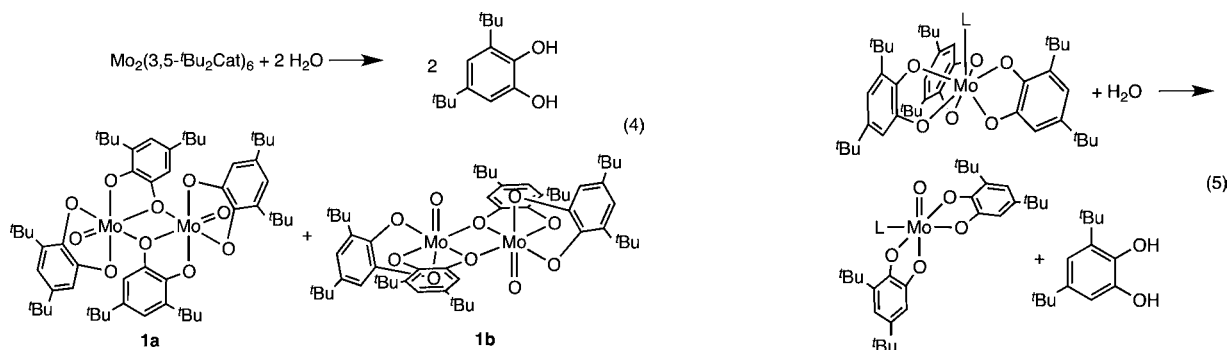


**Figure 3.** Variable-temperature  $^1\text{H}$  NMR spectra of  $(3,5\text{-}^t\text{Bu}_2\text{Cat})_3\text{Mo}(\text{py})$  (500 MHz, toluene- $d_8$ ). x = solvent residual peaks; B =  $\text{C}_6\text{H}_6$ ; ● =  $(3,5\text{-}^t\text{Bu}_2\text{Cat})_3\text{Mo}(\text{py})$ ; ○ = free py.

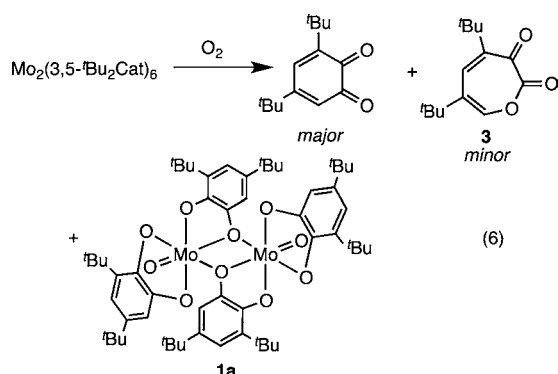


lybdenum dimer  $\text{MoO}(3,5\text{-}^t\text{Bu}_2\text{Cat})(\mu\text{-}3,5\text{-}^t\text{Bu}_2\text{Cat})_2\text{MoO}(3,5\text{-}^t\text{Bu}_2\text{Cat})_2$  (**2**).

The monomeric pyridine-*N*-oxide adduct  $(3,5\text{-}^t\text{Bu}_2\text{Cat})_3\text{Mo}(\text{Opy})$  also reacts immediately with water to form the oxo complex  $(3,5\text{-}^t\text{Bu}_2\text{Cat})_2\text{MoO}(\text{Opy})^6$  and free catechol (eq 5). The pyridine adduct  $(3,5\text{-}^t\text{Bu}_2\text{Cat})_3\text{Mo}(\text{py})$  behaves similarly, except that pyridinium salts of a variety of oxocatecholate anions are formed in addition to the oxo complex  $(3,5\text{-}^t\text{Bu}_2\text{Cat})_2\text{MoO}(\text{py})$ .

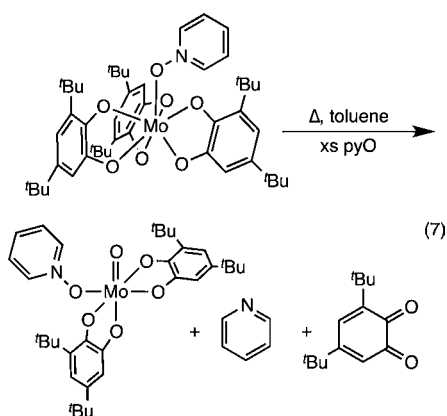
**Oxidations of Tris(catecholate)molybdenum(VI) Complexes.** As originally reported,<sup>7</sup>  $\text{Mo}_2(3,5\text{-}^t\text{Bu}_2\text{Cat})_6$  reacts with  $\text{O}_2$ , albeit more slowly than it reacts with water. The molybdenum-containing product of the reaction with  $\text{O}_2$  (at 1 atm, added via vacuum line to avoid the addition of moisture) is the Buchanan–Pierpont isomer of the oxomolybdenum(VI) dimer  $\text{Mo}_2\text{O}_2(3,5\text{-}^t\text{Bu}_2\text{Cat})_4$  (**1a**); none of the second isomer **1b** observed in the hydrolysis reaction is observed by  $^1\text{H}$  NMR in the oxygenation reaction. The major (68% in  $\text{CDCl}_3$ , 82% in

toluene- $d_8$ ) organic product from the reaction is 3,5-di-*tert*-butyl-1,2-benzoquinone, with the residue consisting of the extradiol oxidation product 4,6-di-*tert*-butyl-1-oxacyclohepta-4,6-diene-2,3-dione (**3**), identified by its  $^1\text{H}$  NMR spectrum<sup>24</sup> (eq 6). At early times in the oxygenation reactions, the same monooxo dimer **2** formed by incomplete hydrolysis of  $\text{Mo}_2(3,5\text{-}^t\text{Bu}_2\text{Cat})_6$  is observed by  $^1\text{H}$  NMR spectroscopy.



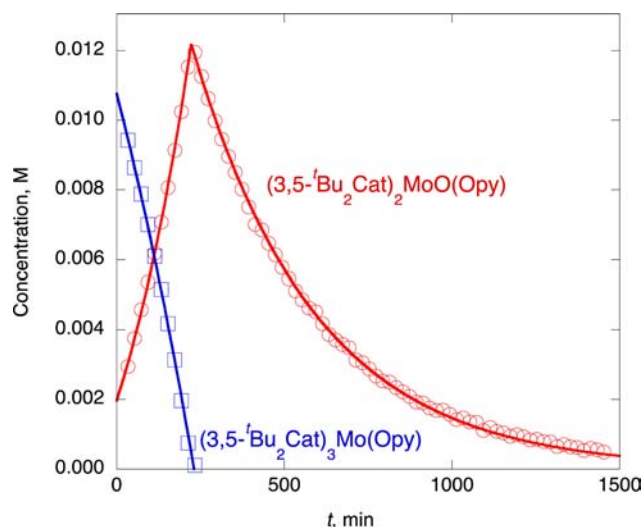
In the presence of pyridine,  $(3,5\text{-}^t\text{Bu}_2\text{Cat})_3\text{Mo}(\text{py})$  reacts with  $\text{O}_2$  to form  $(3,5\text{-}^t\text{Bu}_2\text{Cat})_2\text{MoO}(\text{py})$ . This reaction is substantially slower than the reaction with the homoleptic dimer, suggesting that coordination of  $\text{O}_2$  takes place in the initial stages of the reaction. Pyridine also suppresses formation of the extradiol oxidation product **3**. Quinone is nearly ( $\sim 90\%$ ) the sole organic product of oxygenation in  $\text{CDCl}_3$ ; in toluene- $d_8$ , quinone is the only organic product detectable by  $^1\text{H}$  NMR spectroscopy.

The pyridine-*N*-oxide adduct  $(3,5\text{-}^t\text{Bu}_2\text{Cat})_3\text{Mo}(\text{Opy})$  reacts under anaerobic conditions at elevated temperatures in toluene- $d_8$  in the presence of excess pyridine-*N*-oxide to form 3,5-di-*tert*-butyl-1,2-benzoquinone, free pyridine, and  $(3,5\text{-}^t\text{Bu}_2\text{Cat})_2\text{MoO}(\text{Opy})$  in quantitative yield (eq 7). Once



formed,  $(3,5\text{-}^t\text{Bu}_2\text{Cat})_2\text{MoO}(\text{Opy})$  is itself subject to oxidative degradation as previously described.<sup>6</sup> Thus, all three catecholates of  $(3,5\text{-}^t\text{Bu}_2\text{Cat})_3\text{Mo}(\text{Opy})$  are ultimately converted to quinone, and the molybdenum is mineralized to solid  $\text{MoO}_3(\text{Opy})$ .

The time course of the reaction (Figure 4) shows two peculiarities. First, no  $\text{MoO}_3(\text{Opy})$  is formed until the tris(catecholate) complex  $(3,5\text{-}^t\text{Bu}_2\text{Cat})_3\text{Mo}(\text{Opy})$  is completely consumed; until that point,  $^1\text{H}$  NMR integration against an internal standard shows that the total amount of soluble molybdenum species (the sum of  $(3,5\text{-}^t\text{Bu}_2\text{Cat})_3\text{Mo}(\text{Opy})$  and  $(3,5\text{-}^t\text{Bu}_2\text{Cat})_2\text{MoO}(\text{Opy})$ ) remains constant. Second, reaction

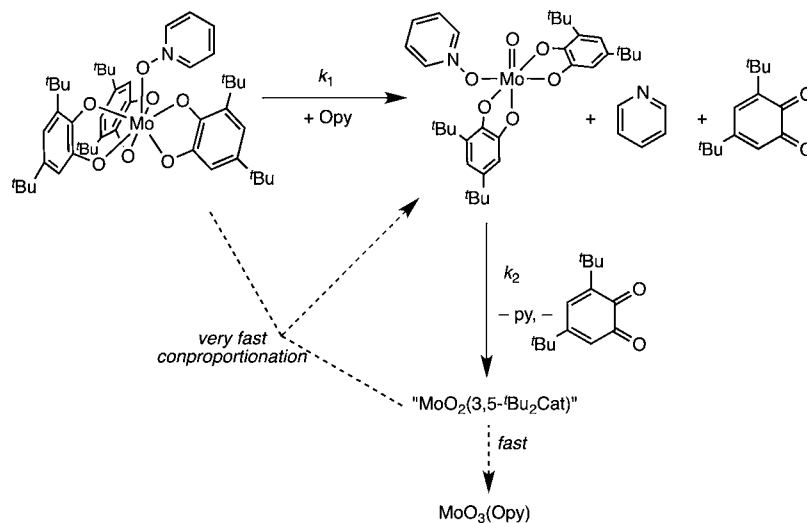


**Figure 4.** Typical time course of reaction of  $(3,5\text{-}^t\text{Bu}_2\text{Cat})_3\text{Mo}(\text{Opy})$  with excess Opy ( $70^\circ\text{C}$ ,  $\text{C}_6\text{D}_5\text{CD}_3$ , total  $[\text{Mo}] = 0.0122\text{ M}$ , total  $[\text{Opy}] = 0.103\text{ M}$ ). Open squares ( $\square$ ) represent  $[(3,5\text{-}^t\text{Bu}_2\text{Cat})_3\text{Mo}(\text{Opy})]$ , open circles ( $\circ$ ) represent  $[(3,5\text{-}^t\text{Bu}_2\text{Cat})_2\text{MoO}(\text{Opy})]$ . Solid lines represent the best fit to Supporting Information, eqs S5 and S6–S7, respectively.

of the tris(catecholate) complex actually accelerates slightly as the reactant is consumed, leading to an abrupt disappearance time for the tris(catecholate). Both of these unusual features can be explained if the initial product of reaction of the oxobis(catecholate) complex, presumably a dioxomolybdenum species  $(3,5\text{-}^t\text{Bu}_2\text{Cat})\text{MoO}_2(\text{Opy})_n$ , conproportionates rapidly with the tris(catecholate) complex  $(3,5\text{-}^t\text{Bu}_2\text{Cat})_3\text{Mo}(\text{Opy})$  to form 2 equiv of oxobis(catecholate)  $(3,5\text{-}^t\text{Bu}_2\text{Cat})_2\text{MoO}(\text{Opy})$  (Scheme 1). Qualitatively, capture of  $(3,5\text{-}^t\text{Bu}_2\text{Cat})\text{MoO}_2(\text{Opy})_n$  by the starting tris(catecholate) complex explains why  $\text{MoO}_3(\text{Opy})$  production is suppressed while any  $(3,5\text{-}^t\text{Bu}_2\text{Cat})_3\text{Mo}(\text{Opy})$  remains. It also explains the accelerated rate of decomposition of  $(3,5\text{-}^t\text{Bu}_2\text{Cat})_3\text{Mo}(\text{Opy})$ , since the tris(catecholate) complex is consumed not only by its own deoxygenation of pyridine-*N*-oxide but also through the reaction of  $(3,5\text{-}^t\text{Bu}_2\text{Cat})_2\text{MoO}(\text{Opy})$ , which is the product of the oxidation of the tris(catecholate). Based on the good mass balance of molybdenum observed by NMR (until  $\text{MoO}_3(\text{Opy})$  begins forming), the proposed dioxo species must have a low steady-state concentration; attempts to generate it by a different route, such as addition of 1 equiv of  $3,5\text{-}^t\text{Bu}_2\text{CatH}_2$  to  $\text{MoO}_2(\text{acac})_2$ , have been unsuccessful.

Since  $(3,5\text{-}^t\text{Bu}_2\text{Cat})_2\text{MoO}(\text{Opy})$  acts as a catalyst for the consumption of  $(3,5\text{-}^t\text{Bu}_2\text{Cat})_3\text{Mo}(\text{Opy})$ , it is reasonable that the reaction shows the accelerated decay typical of autocatalytic reactions. Most autocatalytic reactions retain a first-order dependence on the reactant, giving rise to sigmoidal kinetics.<sup>25</sup> Here, the autocatalytic step is zeroth order in the tris(catecholate) complex, so its decay continues to accelerate until it is fully consumed, giving rise to an abrupt disappearance of the reactant. Quantitatively, the rate equations for this reaction scheme can be integrated exactly (see Supporting Information for details), and the data are well described by this kinetic model (Figure 4).

The kinetics would be equally well described if the monocatecholate intermediate rapidly formed  $\text{MoO}_3(\text{Opy})$  (either by disproportionation or further reaction with pyridine-*N*-oxide), and it was the  $\text{MoO}_3(\text{Opy})$  that conproportionated

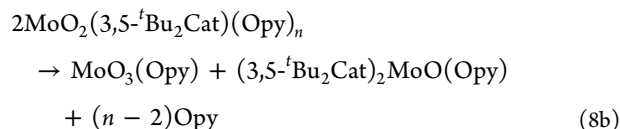
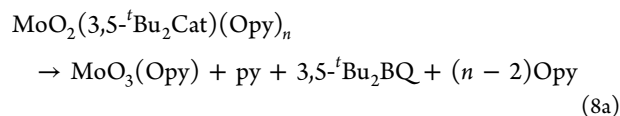
Scheme 1. Proposed Mechanism for Reaction of  $(3,5\text{-}^t\text{Bu}_2\text{Cat})_3\text{Mo}(\text{Opy})$  with Excess Opy

with the tris(catecholato) complex to form the monooxo-bis(catecholato) complex. However, control experiments indicate that neither bulk  $\text{MoO}_3$  nor isolated  $\text{MoO}_3(\text{Opic})^6$  reacts with  $(3,5\text{-}^t\text{Bu}_2\text{Cat})_3\text{Mo}(\text{Opy})$  (in the presence of Opy or Opic) at a significant rate even at  $70^\circ\text{C}$ . While it is possible that a nascent form of  $\text{MoO}_3$  is produced in the reaction that is significantly more reactive than bulk  $\text{MoO}_3$ , it appears more likely that it is a species such as  $\text{MoO}_2(3,5\text{-}^t\text{Bu}_2\text{Cat})(\text{Opy})_n$  that is captured by the tris(catecholato) complex  $(3,5\text{-}^t\text{Bu}_2\text{Cat})_3\text{Mo}(\text{Opy})$ .

At the point where the tris(catecholato) complex  $(3,5\text{-}^t\text{Bu}_2\text{Cat})_3\text{Mo}(\text{Opy})$  disappears, the fate of this dioxo intermediate suddenly changes, from being converted to the monooxo complex  $(3,5\text{-}^t\text{Bu}_2\text{Cat})_2\text{MoO}(\text{Opy})$  to being converted to  $\text{MoO}_3(\text{Opy})$ . At this cusp, almost all of the molybdenum is in the form of the monooxo complex  $(3,5\text{-}^t\text{Bu}_2\text{Cat})_2\text{MoO}(\text{Opy})$ , so its rate of oxygen atom transfer dictates the progress of the reaction. Just before the cusp, each time a mole of  $(3,5\text{-}^t\text{Bu}_2\text{Cat})_2\text{MoO}(\text{Opy})$  undergoes oxygen atom transfer, it produces one mole of benzoquinone and actually makes an *additional* mole of itself (since subsequent capture of the dioxomolybdenum intermediate by the tris(catecholato) reactant makes two moles of the monooxo molybdenum complex).

Immediately after the cusp, the rate of oxygen atom transfer within  $(3,5\text{-}^t\text{Bu}_2\text{Cat})_2\text{MoO}(\text{Opy})$  will be substantially unchanged, since its concentration is almost unchanged, but the rate of formation of products will depend on the route the dioxo intermediate takes to form  $\text{MoO}_3(\text{Opy})$ . If the dioxo complex reacts by further deoxygenation of pyridine-*N*-oxide (eq 8a), then each mole of  $(3,5\text{-}^t\text{Bu}_2\text{Cat})_2\text{MoO}(\text{Opy})$  that undergoes oxygen atom transfer will produce *two* moles of benzoquinone while consuming one mole of the oxo complex. In contrast, if the dioxo intermediate forms  $\text{MoO}_3(\text{Opy})$  by disproportionation (eq 8b), then each mole of  $(3,5\text{-}^t\text{Bu}_2\text{Cat})_2\text{MoO}(\text{Opy})$  that undergoes oxygen atom transfer will produce only *one* mole of benzoquinone (disproportionation produces no quinone) and will result in net consumption of only *one-half* mole of monooxo complex (since each mole of  $\text{MoO}_3(\text{Opy})$  produced is accompanied by restoration of a mole of the monooxo complex). Experimentally, at the cusp, the rate of production of benzoquinone is unchanged and the rate of production of  $(3,5\text{-}^t\text{Bu}_2\text{Cat})_2\text{MoO}(\text{Opy})$  changes abruptly by a

factor of  $-0.5$  (Supporting Information, Figure S3b). This is exactly what is predicted if  $\text{MoO}_3(\text{Opy})$  is formed by disproportionation (eq 8b) and inconsistent with eq 8a.



Quantitative analysis of the experimental time course of the concentration of  $(3,5\text{-}^t\text{Bu}_2\text{Cat})_2\text{MoO}(\text{Opy})$  in toluene at  $70^\circ\text{C}$  gives average values of the rate constant  $k_1 = 3.6(5) \times 10^{-5} \text{ s}^{-1}$  and  $k_2 = 9.4(3) \times 10^{-5} \text{ s}^{-1}$  (triplicate measurements). The latter rate constant is in satisfactory agreement with the rate constant determined independently by UV-visible spectroscopic monitoring of reactions of  $(3,5\text{-}^t\text{Bu}_2\text{Cat})_2\text{MoO}(\text{Opy})^6$  (e.g.,  $k_2 = 1.60(8) \times 10^{-4} \text{ s}^{-1}$  at  $72.5^\circ\text{C}$ ).<sup>26</sup> In the regime where tris(catecholato) is still present, the reactions of both tris- and bis(catecholato) result in disappearance of tris(catecholato), with its rate shifting from  $k_1[\text{Mo}_{\text{total}}]$  initially (when almost all the molybdenum is in the form of  $(3,5\text{-}^t\text{Bu}_2\text{Cat})_3\text{Mo}(\text{Opy})$ ) to  $k_2[\text{Mo}_{\text{total}}]$  at the end of this phase of the reaction (when almost all the molybdenum is in the form of  $(3,5\text{-}^t\text{Bu}_2\text{Cat})_2\text{MoO}(\text{Opy})$ ). The fact that  $k_2$  is greater than  $k_1$  is consistent with the qualitative observation that the decay of the tris(catecholato) complex accelerates over time, and the fact that this acceleration is only modest is consistent with the fact that  $k_2$  is only modestly greater than  $k_1$ .

## DISCUSSION

**Origin of Lewis Acidity of Tris(3,5-di-*tert*-butylcatecholato)molybdenum(VI).** A prominent feature of  $(3,5\text{-}^t\text{Bu}_2\text{Cat})_3\text{Mo}$  is its Lewis acidity, resulting in a tendency to form seven-coordinate adducts with Lewis bases. In the solid state, it dimerizes via catecholato bridges, and the dimeric structure appears to be retained at low temperature in solution. Lewis bases such as pyridine or pyridine-*N*-oxide are bound tightly, with no sign of free  $(3,5\text{-}^t\text{Bu}_2\text{Cat})_3\text{Mo}$  even in the



absence of excess ligand. Monomeric  $(3,5\text{-}^t\text{Bu}_2\text{Cat})_3\text{Mo}$  is likely thermally accessible in solutions of the dimer in non-coordinating solvent, based on the coalescence of all catecholate resonances into a single environment at  $\sim 30^\circ\text{C}$ , and the monomeric complex is certainly thermally accessible from  $(3,5\text{-}^t\text{Bu}_2\text{Cat})_3\text{Mo}(\text{py})$ , based on its dissociative mechanism of ligand substitution. Nevertheless, the enthalpy of activation for dissociation of pyridine ( $\Delta H_{\text{diss}}^\ddagger = 15.4 \pm 0.6$  kcal/mol) provides evidence for the appreciable Lewis acidity of the six-coordinate tris(catecholate).

Electronically, monomeric octahedral tris(catecholato)molybdenum(VI) would best be considered a 16-electron complex. Catecholate has one strongly  $\pi$ -donating orbital, the in-phase combination of oxygen  $p\pi$  lone pairs, which is raised in energy because of its antibonding interaction with one of the filled benzene  $\pi$  orbitals.<sup>27</sup> Taken in addition to the six  $\sigma$  bonds,  $\pi$  donation from the three ligands would saturate the molybdenum center. However, the  $a_2$ -symmetric combination of ligand  $\pi$  donor orbitals finds no symmetry match among the metal d orbitals (which transform as  $a_1 + 2e$  in  $D_3$  symmetry).<sup>28</sup> This leaves the  $d_z^2$  orbital (taking the  $z$  axis along the molecular 3-fold axis, this is a  $d\pi$  orbital) as essentially nonbonding and thus available for binding to a seventh ligand.

Previously prepared molybdenum tris(catecholate) complexes have also shown signs of electron deficiency. For example, in the solid state, one of the ligands in  $\text{Mo}(\text{phenanthrorenediolate})_3$  adopts an  $\eta^4$  geometry,<sup>29</sup> with the Mo–C distances (2.421–2.426 Å) similar to analogous ones in  $\text{Mo}(\eta^4\text{-}2,3\text{-butadiene})_3$  (2.393–2.404 Å).<sup>30</sup> This effectively makes the molybdenum seven-coordinate. Molybdenum(VI) tris(tetrachlorocatecholate) adopts a dimeric structure with two bridging catecholates which bind in a  $\kappa^1, \kappa^1$  fashion;<sup>31</sup> the tungsten analogue is isostructural.<sup>32</sup> While the molybdenum remains six-coordinate, the bridging catecholates are able to bind with much more obtuse Mo–O–C angles than the chelating ligands ( $134(5)^\circ$  vs  $118.4(10)^\circ$  avg). Increasing the M–O–C angle is known to allow for enhanced  $\pi$  donation,<sup>33</sup> and indeed the bridging catecholates show significantly shorter Mo–O distances than the chelating ones (1.861(11) Å vs 1.948(10) Å). A similar argument has been adduced to explain the preference for monodentate aryloxide donation over catecholate chelation in the (diketonate)<sub>2</sub>Ti(IV) fragment isoelectronic with  $(\text{Cl}_4\text{C}_6\text{O}_2)_2\text{Mo}(\text{VI})$ .<sup>34</sup> Thus, although formation of adducts with exogenous bases has not been previously reported, Lewis acidity appears to be a general feature of tris(catecholate)molybdenum complexes.

The Lewis acidity of tris(catecholate)molybdenum contrasts with the behavior of the lighter congener, chromium, where  $(\text{R}_4\text{C}_6\text{O}_2)_3\text{Cr}$  complexes are invariably octahedral tris(chelates).<sup>35</sup> This is undoubtedly due in part to the smaller size of chromium, which makes seven-coordination less favorable, but electronic factors also likely play a role. Because of the lower d-orbital energy of Cr compared to Mo, neutral tris(catecholato)chromium species are best described as Cr(III) complexes of semiquinonate ligands, with strong antiferromagnetic coupling giving rise to an  $S = 0$  ground state.<sup>36</sup> The orbitals derived from the Cr  $d_z^2$  are thus not empty, and the metal is correspondingly not electrophilic. An analogous effect is observed in tris(benzenedithiolate)molybdenum complexes, where the orbital energy of the ligands is raised because of the lower electronegativity of sulfur compared to oxygen. Again the  $d_z^2$  orbital has significant electron density, due either to formal electron transfer to Mo (the complexes have been described as

containing Mo(V)<sup>37</sup> or Mo(IV)<sup>38</sup>) or to donation from the ligand  $\pi$  orbitals enabled by ligand folding and reduction in symmetry of the trigonal prismatic geometry to  $C_{3h}$ .<sup>39</sup> Again the complexes are isolated as six-coordinate monomers, though they are known to react under some conditions with nucleophiles.<sup>40</sup>

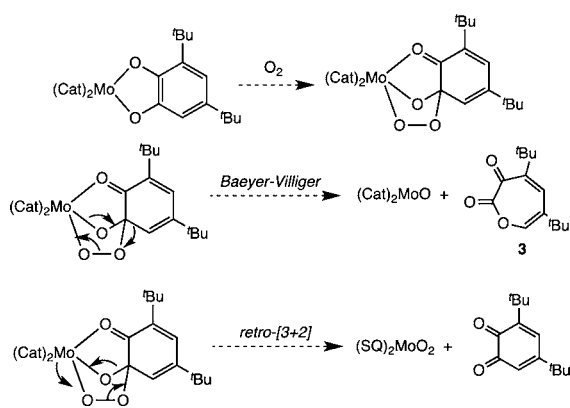
**Nonclassical Redox Reactions of  $(3,5\text{-}^t\text{Bu}_2\text{Cat})_3\text{Mo}$ .** In an earlier study of  $(3,5\text{-}^t\text{Bu}_2\text{Cat})_2\text{Mo}(\text{O})(\text{Opy})$ , it was found that the oxomolybdenum(VI) bis(catecholate) fragment deoxygenated pyridine-*N*-oxide form 3,5-di-*tert*-butyl-1,2-benzoquinone and, ultimately,  $\text{MoO}_3(\text{Opy})$ .<sup>6</sup> Because the oxygen atom was delivered to the molybdenum, while the electrons needed for reducing the *N*-oxide were drawn from coordinated catecholate, this mode of reactivity was described as a “nonclassical” oxygen atom transfer reaction. Since  $(3,5\text{-}^t\text{Bu}_2\text{Cat})_3\text{Mo}(\text{Opy})$  also has coordinated pyridine-*N*-oxide, coordinated catecholate, and molybdenum(VI) to mediate between them, it was of interest to assess the ability of the molybdenum tris(catecholate) fragment to undergo nonclassical oxygen atom transfer as well.

The tris(catecholate) complex  $(3,5\text{-}^t\text{Bu}_2\text{Cat})_3\text{Mo}(\text{Opy})$  does react cleanly in the presence of excess *Opy* to form  $(3,5\text{-}^t\text{Bu}_2\text{Cat})_2\text{Mo}(\text{O})(\text{Opy})$ , free pyridine, and 3,5-*t*-Bu<sub>2</sub>BQ. In the absence of a detailed mechanistic study, we cannot absolutely rule out the possibility of quinone dissociation prior to N–O bond cleavage. However, since the reaction is not inhibited by benzoquinone and is very sensitive to the nature of the oxidant (*N*-methylmorpholine-*N*-oxide reacts in minutes at room temperature), it seems likely that the tris(catecholate) reacts by an analogous mechanism to the bis(catecholate) species, that is, by initial N–O bond cleavage to form an oxomolybdenum species with oxidized catecholates, followed by subsequent dissociation of quinone. This nonclassical oxygen atom transfer mechanism would require the formation of a short-lived seven-coordinate oxotris(dioxolene) species. The isolation of  $(3,5\text{-}^t\text{Bu}_2\text{Cat})_3\text{Mo}(\text{py})$  indicates that this is sterically accessible, and while seven-coordinate molybdenum(VI) oxo complexes are uncommon (except for complexes with peroxy or related ligands), they are preceded with small bite angle ligands such as dithiocarbamates.<sup>41</sup>

The reactivity of the tris(catecholate)molybdenum fragment toward pyridine-*N*-oxide is strikingly similar to that of the oxobis(catecholate)molybdenum fragment, with rate constants for the reaction of the former and latter species differing by less than an order of magnitude at  $70^\circ\text{C}$  in toluene. The reaction of  $(3,5\text{-}^t\text{Bu}_2\text{Cat})_3\text{Mo}(\text{Opy})$  with excess pyridine-*N*-oxide constitutes a net *six*-electron process, ultimately producing  $\text{MoO}_3(\text{Opy})$  and 3 equiv of 3,5-di-*tert*-butyl-1,2-benzoquinone. Not only is it unusual to find metal centers that can span such a wide range of oxidation states, but if one does, then successive one- or two-electron steps often occur at highly disparate rates since successive redox potentials typically change dramatically as the metal oxidation state changes. In the present system, each successive two-electron transformation involves the same catecholate to quinone oxidation, so it is perhaps not surprising that the first and second oxidations occur at similar rates. (The third oxidation step is obscured by fast disproportionation of the putative dioxomonocatecholate species.) The ability demonstrated here of multiple redox-active ligands to supply large numbers of electrons at relatively similar rates illustrates two potential advantages of a nonclassical oxidation strategy for achieving multielectron redox chemistry.

In contrast to their similar reactivity toward pyridine-*N*-oxide, the tris(catecholato)molybdenum and oxobis(catecholato)molybdenum fragments behave very differently toward dioxygen. The tris(catecholato) complexes  $(3,5\text{-}^t\text{Bu}_2\text{Cat})_3\text{Mo(L)}$  or dimeric  $\text{Mo}_2(3,5\text{-}^t\text{Bu}_2\text{Cat})_6$  are readily oxidized by  $\text{O}_2$ , with reactions proceeding rapidly even at room temperature, while  $(3,5\text{-}^t\text{Bu}_2\text{Cat})_2\text{MoO(L)}$  or dimeric  $\text{Mo}_2\text{O}_2(3,5\text{-}^t\text{Bu}_2\text{Cat})_4$  are air-stable. When dioxygen reacts, it affords significant amounts of the extradiol oxidation product 4,6-di-*tert*-butyl-1-oxacyclohepta-4,6-diene-2,3-dione (**3**), as well as the quinone which is the exclusive product of oxidations with pyridine-*N*-oxide. Ring-expanded products like **3** are usually attributed to Baeyer–Villiger ring expansions of peroxyquinone intermediates (e.g., Scheme 2). Similar

**Scheme 2. Possible Intermediacy of Peroxyquinones in Formation of **3** and Quinone**



intermediates derived from iminoquinones have been observed directly in other reactions of dioxygen with catecholato or amidophenoxide complexes of redox-inert metals.<sup>42</sup> The observation that donors such as pyridine retard the reaction suggests that  $\text{O}_2$  must find an open coordination site on Mo to react. The effect of pyridine on the product distribution (suppressing formation of extradiol oxidation) is more difficult to interpret. One possibility is that pyridine affects the selectivity of fragmentation of the peroxyquinone intermediate, enhancing quinone formation or inhibiting Baeyer–Villiger rearrangement. Alternatively, the metal might also react with  $\text{O}_2$  by a pathway that does not involve C–O bond formation, and pyridine might favor this pathway at the expense of forming the peroxyquinone intermediate. Even with the limited data available, it is clear that the reactivity of dioxygen does not parallel that of simple two-electron oxygen atom donors such as pyridine-*N*-oxide.

## CONCLUSIONS

The tris(catecholato)molybdenum(VI) fragment  $[(3,5\text{-}^t\text{Bu}_2\text{Cat})_3\text{Mo}]$  is Lewis acidic, existing in the solid state and in noncoordinating solvents as a seven-coordinate dimer with bridging catecholates. Lewis bases add to give seven-coordinate monomers such as capped octahedral  $(3,5\text{-}^t\text{Bu}_2\text{Cat})_3\text{Mo(py)}$ . These compounds are well described as containing Mo(VI) and dianionic catecholates, with significant  $\pi$  donation from the catecholates to the molybdenum. The reducing power stored in the catecholato ligands can be harnessed in reactions with pyridine-*N*-oxide (which forms exclusively 3,5-di-*tert*-butyl-1,2-benzoquinone)

and dioxygen (which forms both quinone and the extradiol oxidation product 4,6-di-*tert*-butyl-1-oxacyclohepta-4,6-diene-2,3-dione). The metal center appears to play a critical role in both cases in binding the oxidant as well as serving as the ultimate acceptor of oxygen atoms from the oxidant, forming oxomolybdenum(VI) species as products. The molybdenum maintains its +6 oxidation state throughout the reactions. The reaction with pyridine-*N*-oxide is thus a “nonclassical” oxygen atom transfer reaction, in which the oxygen atom is delivered to the metal center but the electrons needed to reduce the *N*-oxide come from the catecholato. The reaction with dioxygen is likely more complicated, as the presence of an extradiol oxidation product strongly suggests that the catecholato serves not only as a reservoir of electrons but also engages in formation of new covalent bonds to the  $\text{O}_2$  substrate over the course of the reaction.

## ASSOCIATED CONTENT

### Supporting Information

Eyring plot for exchange of free and bound pyridine in  $(3,5\text{-}^t\text{Bu}_2\text{Cat})_3\text{Mo(py)}$ , van't Hoff plot of eq 3, plots of  $^1\text{H}$  NMR spectra and time evolution of species in the thermolysis of  $(3,5\text{-}^t\text{Bu}_2\text{Cat})_3\text{Mo(Opy)}$ , and derivation of kinetic equations for the thermolysis of  $(3,5\text{-}^t\text{Bu}_2\text{Cat})_3\text{Mo(Opy)}$  (PDF format) and crystallographic information on  $\text{Mo}_2(3,5\text{-}^t\text{Bu}_2\text{Cat})_6\cdot 4\text{C}_6\text{D}_6$  and  $(3,5\text{-}^t\text{Bu}_2\text{Cat})_3\text{Mo(py)}\cdot\text{CH}_3\text{CN}$  in CIF format. This material is available free of charge via the Internet at <http://pubs.acs.org>.

## AUTHOR INFORMATION

### Corresponding Author

\*E-mail: Seth.N.Brown.114@nd.edu.

### Notes

The authors declare no competing financial interest.

## ACKNOWLEDGMENTS

We thank Dr. Allen Oliver for assistance with the X-ray crystallography and Prof. Richard G. Finke for helpful discussions about autocatalysis. This work was supported by the National Science Foundation (CHE-1112356). K.R. acknowledges summer fellowship support from the Notre Dame RESACC program.

## REFERENCES

- (1) (a) Pierpont, C. G.; Lange, C. W. *Prog. Inorg. Chem.* **1994**, *41*, 331–442. (b) Pierpont, C. G. *Coord. Chem. Rev.* **2001**, *219–221*, 415–433.
- (2) (a) Costas, M.; Mehn, M. P.; Jensen, M. P.; Que, L., Jr. *Chem. Rev.* **2004**, *104*, 939–986. (b) Vaillancourt, F. H.; Bolin, J. T.; Eltis, L. D. *Crit. Rev. Biochem. Mol. Biol.* **2006**, *41*, 241–267.
- (3) Yin, C.-X.; Finke, R. G. *J. Am. Chem. Soc.* **2005**, *127*, 9003–9013.
- (4) Morris, A. M.; Pierpont, C. G.; Finke, R. G. *J. Mol. Catal. A* **2009**, *309*, 137–145.
- (5) Munhá, R. F.; Zarkesh, R. A.; Heyduk, A. F. *Dalton Trans.* **2013**, *42*, 3751–3766.
- (6) Marshall-Roth, T.; Liebscher, S. C.; Rickert, K.; Seewald, N. J.; Oliver, A. G.; Brown, S. N. *Chem. Commun.* **2012**, *48*, 7826–7828.
- (7) Cass, M. E.; Pierpont, C. G. *Inorg. Chem.* **1986**, *25*, 122–123.
- (8) Buchanan, R. M.; Pierpont, C. G. *Inorg. Chem.* **1979**, *18*, 1616–1620.
- (9) Budzelaar, P. H. M. *gNMR*, v. 3.5.6; Cherwell Scientific Publishing: Oxford, U.K., 1996.
- (10) Sheldrick, G. M. *Acta Crystallogr., Sect. A* **2008**, *A64*, 112–122.

- (11) *International Tables for Crystallography*; Kluwer Academic Publishers: Dordrecht, The Netherlands, 1992; Vol C.
- (12) Calucci, L.; Pampaloni, G.; Pinzino, C.; Prescimone, A. *Inorg. Chim. Acta* **2006**, *359*, 3911–3920.
- (13) (a) Borgias, B. A.; Cooper, S. R.; Koh, Y. B.; Raymond, K. N. *Inorg. Chem.* **1984**, *23*, 1009–1016. (b) Shoner, S. C.; Power, P. P. *Inorg. Chem.* **1992**, *31*, 1001–1010. (c) Speier, G.; Tisza, S.; Tyeklar, Z.; Lange, C. W.; Pierpont, C. G. *Inorg. Chem.* **1994**, *33*, 2041–2045. (d) Chi, Y.; Lan, J.-W.; Ching, W.-L.; Peng, S.-M.; Lee, G.-H. *J. Chem. Soc., Dalton Trans.* **2000**, 2923–2927. (e) Manos, M. J.; Tasiopoulos, A. J.; Raptopoulou, C.; Terzis, A.; Woollins, J. D.; Slawin, A. M. Z.; Keramidis, A. D.; Kabanos, T. A. *J. Chem. Soc., Dalton Trans.* **2001**, 1556–1558. (f) Fukin, G. K.; Zakharov, L. N.; Maslennikov, S. V.; Piskunov, A. V.; Cherkasov, V. K. *Acta Crystallogr., Sect. C* **2001**, *57*, 1020–1021. (g) Kaizer, J.; Pap, J.; Speier, G.; Párkányi, L.; Korecz, L.; Rockenbauer, A. *J. Inorg. Biochem.* **2002**, *91*, 190–198. (h) Banse, F.; Bolland, V.; Philouze, C.; Rivière, E.; Tchertanova, L.; Girerd, J.-J. *Inorg. Chim. Acta* **2003**, *353*, 223–230. (i) Boudalis, A. K.; Dahan, F.; Bousseksou, A.; Tuchagues, J.-P.; Perlepes, S. P. *Dalton Trans.* **2003**, 3411–3418. (j) Maslennikov, S. V.; Aivaz'yan, I. A.; Fukin, G. K.; Cherkasov, V. K.; Kurskii, Y. A. *Koord. Khim.* **2004**, *30*, 667–672. (k) Davidson, M. G.; Jones, M. D.; Lunn, M. D.; Mahon, M. F. *Inorg. Chem.* **2006**, *45*, 2282–2287. (l) Wagner, M.; Limberg, C.; Tietz, T. *Chem.—Eur. J.* **2009**, *15*, 5567–5576. (m) Scales, E.; Sorace, L.; Dei, A.; Caneschi, A.; Muryn, C. A.; Collison, D.; McInnes, E. J. L. *Chem. Sci.* **2010**, *1*, 221–225. (n) Flogeras, J. C.; Allan, C. R.; Vogels, C. M.; Decken, A.; Westcott, S. A. *X-ray Struct. Anal. Online* **2011**, *27*, 45–46.
- (14) (a) Block, E.; Ofori-Okai, G.; Kang, H.; Zubieta, J. *Inorg. Chim. Acta* **1991**, *190*, 179–184. (b) Hughes, D. L.; Lazarowych, N. J.; Maguire, M. J.; Morris, R. H.; Richards, R. L. *J. Chem. Soc., Dalton Trans.* **1995**, 5–15. (c) Sukcharoenphon, K.; Capps, K. B.; Abboud, K. A.; Hoff, C. D. *Inorg. Chem.* **2001**, *40*, 2402–2408. (d) Yonemura, T.; Nakata, J.; Kadota, M.; Hasegawa, M.; Okamoto, K.; Ama, T.; Kawaguchi, H.; Yasui, T. *Inorg. Chem. Commun.* **2001**, *4*, 661–663. (e) Yonemura, T.; Hashimoto, T.; Hasegawa, M.; Ikenoue, T.; Ama, T.; Kawaguchi, H. *Inorg. Chem. Commun.* **2006**, *9*, 183–186. (f) Yonemura, T. *Acta Crystallogr., Sect. E* **2009**, *65*, m1463–m1464.
- (15) (a) Seymore, S. B.; Brown, S. N. *Inorg. Chem.* **2006**, *45*, 9540–9550. (b) Seymore, S. B.; Brown, S. N. *Inorg. Chem.* **2002**, *41*, 462–469. (c) Seymore, S. B.; Brown, S. N. *Inorg. Chem.* **2001**, *40*, 6676–6683. (d) Bishop, M. W.; Chatt, J.; Dilworth, J. R.; Dahlstrom, P.; Hyde, J.; Zubieta, J. *J. Organomet. Chem.* **1981**, *213*, 109–124. (e) Williams, G. A.; Smith, A. R. P. *Aust. J. Chem.* **1980**, *33*, 717–728. (f) Hursthouse, M. B.; Motevalli, M. *J. Chem. Soc., Dalton Trans.* **1979**, 1362–1366. (g) Butler, G.; Chatt, J.; Hussain, W.; Leigh, G. J.; Hughes, D. L. *Inorg. Chim. Acta* **1978**, *30*, L287–L288.
- (16) (a) Bristow, S.; Enemark, J. H.; Garner, C. D.; Minelli, M.; Morris, G. A.; Ortega, R. B. *Inorg. Chem.* **1985**, *24*, 4070–4077. (b) Bristow, S.; Garner, C. D.; Morris, G. A.; Enemark, J. H.; Minelli, M.; Ortega, R. B. *Polyhedron* **1986**, *5*, 319–321.
- (17) Drew, M. G. B. *Prog. Inorg. Chem.* **1977**, *23*, 67–210.
- (18) Kopec, J. A.; Shekar, S.; Brown, S. N. *Inorg. Chem.* **2012**, *51*, 1239–1250.
- (19) Brown, S. N. *Inorg. Chem.* **2012**, *51*, 1251–1260.
- (20) Liu, C.-M.; Nordlander, E.; Schmeh, D.; Shoemaker, R.; Pierpont, C. G. *Inorg. Chem.* **2004**, *43*, 2114–2124.
- (21) (a) Blatchford, T. P.; Chisholm, M. H.; Huffman, J. C. *Inorg. Chem.* **1988**, *27*, 2059–2070. (b) Gosink, H.-J.; Roesky, H. W.; Noltemeyer, M.; Schmidt, H.-G.; Freire-Erdbrugger, C.; Sheldrick, G. M. *Chem. Ber.* **1993**, *126*, 279–283. (c) Feher, F. J.; Rahimian, K.; Budzichowski, T. A.; Ziller, J. W. *Organometallics* **1995**, *14*, 3920–3926. (d) Zhu, S. S.; Cefalo, D. R.; La, D. S.; Jamieson, J. Y.; Davis, W. M.; Hoveyda, A. H.; Schrock, R. R. *J. Am. Chem. Soc.* **1999**, *121*, 8251–8259. (e) Alexander, J. B.; Schrock, R. R.; Davis, W. M.; Hultsch, K. C.; Hoveyda, A. H.; Houser, J. H. *Organometallics* **2000**, *19*, 3700–3715. (f) Hanna, T. A.; Ghosh, A. K.; Ibarra, C.; Mendez-Rojas, M. A.; Rheingold, A. L.; Watson, W. H. *Inorg. Chem.* **2004**, *43*, 1511–1516. (g) Jiang, A. J.; Schrock, R. R.; Müller, P. *Organometallics* **2008**, *27*, 4428–4438.
- (22) This reaction has been reported as a preparation of  $\text{Mo}_2\text{O}_2(3,5\text{-}^i\text{Bu}_2\text{Cat})_4$ , and the dimeric structure in noncoordinating solvents was confirmed by osmometry, but NMR data were only obtained in coordinating solvents in which the complex forms monomeric  $\text{MoO}(3,5\text{-}^i\text{Bu}_2\text{Cat})_2(\text{L})$ , which does not address the question of isomerism in the dimer. Wilshire, J. P.; Leon, L.; Bosserman, P.; Sawyer, D. T. *J. Am. Chem. Soc.* **1979**, *101*, 3379–3381. (23) Cass, M. E.; Greene, D. L.; Buchanan, R. M.; Pierpont, C. G. *J. Am. Chem. Soc.* **1983**, *105*, 2680–2686.
- (24) (a) Funabiki, T.; Mizoguchi, A.; Sugimoto, T.; Tada, S.; Tsuji, M.; Sakamoto, H.; Yoshida, S. *J. Am. Chem. Soc.* **1986**, *108*, 2921–2932. (b) Weiner, H.; Finke, R. G. *J. Am. Chem. Soc.* **1999**, *121*, 9831–9842.
- (25) Watzky, M. A.; Finke, R. G. *J. Am. Chem. Soc.* **1997**, *119*, 10382–10400.
- (26) The values reported in ref 6 are multiplied by two for comparison with the value reported here to account for the fact that oxidation of one mole of  $(3,5\text{-}^i\text{Bu}_2\text{Cat})_2\text{MoO}(\text{Opy})$  results in the disappearance of only one-half a mole of the complex (since disproportionation of the initial product as described in eq 8b restores half a mole of monooxo complex). Thus the apparent decay constants reported in ref 6 correspond to  $0.5k_2$ .
- (27) Gordon, D. J.; Fenske, R. F. *Inorg. Chem.* **1982**, *21*, 2907–2915.
- (28) (a) Karpishin, T. B.; Gebhard, M. S.; Solomon, E. I.; Raymond, K. N. *J. Am. Chem. Soc.* **1991**, *113*, 2977–2984. (b) Karpishin, T. B.; Dewey, T. M.; Raymond, K. N. *J. Am. Chem. Soc.* **1993**, *115*, 1842–1851.
- (29) Pierpont, C. G.; Buchanan, R. M. *J. Am. Chem. Soc.* **1975**, *97*, 4912–4917.
- (30) (a) Bogdanović, B.; Bönnemann, H.; Goddard, R.; Startsev, A.; Wallis, J. M. *J. Organomet. Chem.* **1986**, *299*, 347–355. (b) Yun, S. S.; Kang, S. K.; Suh, I.-H.; Choi, Y. D.; Chang, I. S. *Organometallics* **1991**, *10*, 2509–2512.
- (31) Pierpont, C. G.; Downs, H. H. *J. Am. Chem. Soc.* **1975**, *97*, 2123–2127.
- (32) deLearie, L. A.; Pierpont, C. G. *Inorg. Chem.* **1988**, *27*, 3842–3845.
- (33) Smith, G. D.; Fanwick, P. E.; Rothwell, I. P. *Inorg. Chem.* **1990**, *29*, 3221–3226.
- (34) Dulatas, L. T.; Brown, S. N.; Ojomo, E.; Noll, B. C.; Cavo, M. J.; Holt, P. B.; Wopperer, M. M. *Inorg. Chem.* **2009**, *48*, 10789–10799.
- (35) (a) Pierpont, C. G.; Downs, H. H. *J. Am. Chem. Soc.* **1976**, *98*, 4834–4838. (b) Sofen, S. R.; Ware, D. C.; Cooper, S. R.; Raymond, K. N. *Inorg. Chem.* **1979**, *18*, 234–239. (c) Chang, H.-C.; Kitagawa, S. *Mol. Cryst. Liq. Cryst.* **2002**, *376*, 275–282.
- (36) Kapre, R. R.; Bothe, E.; Weyhermüller, T.; George, S. D.; Muresan, N.; Wieghardt, K. *Inorg. Chem.* **2007**, *46*, 7827–7839.
- (37) Kapre, R. R.; Bothe, E.; Weyhermüller, T.; George, S. D.; Wieghardt, K. *Inorg. Chem.* **2007**, *46*, 5642–5650.
- (38) Tenderholt, A. L.; Szilagy, R. K.; Holm, R. H.; Hodgson, K. O.; Hedman, B.; Solomon, E. I. *Inorg. Chem.* **2008**, *47*, 6382–6392.
- (39) Campbell, S.; Harris, S. *Inorg. Chem.* **1996**, *35*, 3285–3288.
- (40) Cervilla, A.; Pérez-Plá, F.; Llopis, E.; Piles, M. *Dalton Trans.* **2004**, 1461–1465.
- (41) (a) Dirand, J.; Ricard, L.; Weiss, R. *Transition Met. Chem.* **1975**, *1*, 2–5. (b) Dirand, J.; Ricard, L.; Weiss, R. *J. Chem. Soc., Dalton Trans.* **1976**, 278–282. (c) Marabella, C. P.; Enemark, J. H.; Newton, W. E.; McDonald, J. W. *Inorg. Chem.* **1982**, *21*, 623–627. (d) Arzumianian, H.; Corao, C.; Krentzien, H.; Lopez, R.; Teruel, H. *Chem. Commun.* **1992**, 856–858. (e) Decoster, M.; Conan, F.; LeMest, Y.; Pala, J. S.; Leblanc, A.; Molinie, P.; Faulques, E.; Toupet, L. *New J. Chem.* **1997**, *21*, 215–221.
- (42) (a) Abakumov, G. A.; Poddel'sky, A. I.; Grunova, E. V.; Cherkasov, V. K.; Fukin, G. K.; Kurskii, Y. A.; Abakumova, L. G. *Angew. Chem., Int. Ed.* **2005**, *44*, 2767–2771. (b) Cherkasov, V. K.; Abakumov, G. A.; Grunova, E. V.; Poddel'sky, A. I.; Fukin, G. K.; Baranov, E. V.; Kurskii, Y. V.; Abakumova, L. G. *Chem.—Eur. J.* **2006**, *12*, 3916–3927. (c) Poddel'sky, A. I.; Vavilina, N. N.; Somov, N. V.; Cherkasov, V. K.; Abakumov, G. A. *J. Organomet. Chem.* **2009**, *694*,

3462–3469. (d) Poddel'sky, A. I.; Kurskii, Y. A.; Piskunov, A. V.; Somov, N. V.; Cherkasov, V. K.; Abakumov, G. A. *Appl. Organomet. Chem.* **2011**, *25*, 180–189.